International Journal of Digital Twin Systems and Computing (IJDTSC) ISSN:(3108-0790)
Doi: https://doi.org/10.XXXXX/IJDTSC.2025.V1I101

Grid-Connected PV-Wind System with Energy Storage and Electric Vehicle Integration

[1]Ravi Kant Sharma
[1]Indian Institute of Technology, Guwahati
[1]Email id. ravi.sharma@iitg.ac.in

Abstract*—The addition of renewable energy sources into power systems is essential to meet growing energy demands while reducing environmental impact. This study presents an innovative approach to enhancing power generation and optimizing power quality in a grid-connected hybrid system comprising photovoltaic (PV), wind energy, energy storage, and electric vehicle (EV) integration. An Adaptive Neuro-Fuzzy Inference System (ANFIS)-based Maximum Power Point Tracking (MPPT) algorithm is employed to maximize energy harvesting from the PV and wind subsystems under varying environmental conditions. The proposed system also incorporates energy storage to ensure reliability and stability by mitigating fluctuations in renewable energy output. Additionally, the bidirectional interaction with EVs enables energy balancing during peak and off-peak hours. Simulation results demonstrate the system's ability to achieve efficient power management, with reduced Total Harmonic Distortion (THD) of 3.08 % and improved voltage regulation during grid disturbances. The ANFIS-MPPT algorithm exhibits superior performance providing efficiency of 99.5%, ensuring rapid convergence to the optimal operating point. This comprehensive approach highlights the potential of hybrid renewable systems with advanced MPPT techniques and energy storage in delivering enhanced power quality and system reliability, paving the way for sustainable and efficient energy utilization in modern grids.

***Keywords*—:** *Grid-Connected System, PV-Wind Hybrid, Energy Storage, Electric Vehicle Integration, ANFIS MPPT, Power Quality, Total Harmonic Distortion.*

I. INTRODUCTION

Addressing environmental issues and securing a sustainable energy future are the driving forces behind the growing use of renewable energy sources. With their complementing qualities, hybrid systems that combine wind and PV energy provide a viable way to generate power consistently and dependably. But because these energy sources are inherently variable, improving power output and preserving grid stability requires sophisticated management and optimization strategies. Additionally, combining energy storage with EVs increases the possibility of enhancing demand-side management and energy dependability.

An energy management system was introduced in [1] for a hybrid system that included grid-supported battery storage, PV, wind turbines, and EVs connected to residential buildings. Using LSTM models, energy prediction is accomplished with around 95% accuracy using nonlinear programming and sequential quadrature programming. Storage cooperation rates are further optimized using KNN, RF, and GRU regressors, which provide R2 values of 0.6953, 0.8381, and 0.739, respectively. Combining these techniques enables accurate energy management and effective hybrid architecture switching control. A GA-ANFIS controller for PV-wind hybrid microgrid voltage regulation is introduced in [2]. When it comes to rising time, settling time, overshoot, and managing non-linearities, the controller performs better than SSR-P&O and PID controllers, making it an excellent MPPT algorithm. Improved stability and efficiency are demonstrated by the method, which may eventually be included into hybrid AI-based control systems. In [3], a microgrid with PV, DFIG, and fuel cells is discussed, including a battery to reduce intermittency. While MPPT-based ANFIS maximizes PV power extraction, the lack of a PV converter lowers expenses. Grid integration and system stability are improved via droop control and VSG controllers. The efficiency and cost-effectiveness of this novel design are confirmed by simulation results. In [4], a 60kW hybrid PV-wind system with an MPPT controller based on ANFIS is demonstrated. During microgrid integration, the smart controller increases efficiency and stabilizes the system. When fuzzy, ANN, and ANFIS controllers are compared, the higher performance of ANFIS is demonstrated. This system highlights how intelligent controllers help advance the integration of renewable energy sources into microgrids. A neuro-fuzzy control strategy for a wind-powered DFIG combined with an ANN-controlled solar PV array was presented in [5]. The system uses a 30-neuron ANN structure that is tuned for low error to enable maximum power harvesting. The significance of solar integration for lowering system costs and enhancing

dependability is shown by a comparison of wind-solar and wind-only DFIG systems.[6] uses an islanded renewable energy microgrid to solve the electricity need in Luxmanda community, Tanzania. The microgrid runs at a constant 750 V DC and combines PV, wind power, and a DC grid. The suggested grid connection approach highlights the significance of renewable energy in resolving issues with energy access while working to improve power supply and promote rural development.

By removing the need for redundant converters, the combination of hybrid PV-Wind systems with BESS, FC, and Electrolyzer provides an economical option [7]. By using a GSC to optimize PV power injection and a RSC for grid load sharing, the suggested system guarantees energy stability. A lead compensator improves controller stability, while an electrolyzer for hydrogen production solves renewable intermittency. In comparison to traditional systems, MATLAB Simulink findings confirm the system's effectiveness in energy management and consistent power flow.

In [8], an SMC strategy for Hybrid scheme comprising solar and wind energy sources were discussed. By directly linking the PV schemes to the DC-bus, the system reduces component redundancy and improves efficiency. The proposed control ensures stability under varying conditions and proves asymptotic stability using the Lyapunov function. Simulation results validate its robust performance and effective energy management. [9] introduces an optimization structure for a PV linked EV station with energy sharing. The model prioritizes reliability, profitability, and minimal operational costs by considering dynamic energy demand and pricing. Real-world case studies demonstrate significant cost reductions and a short payback period, showcasing the feasibility and economic advantages of the proposed system. [10] focuses on optimizing PV-Wind systems with battery storage for NZEBs. By incorporating total energy transfer (TET) minimization as an objective, the study reduces grid dependency and energy export/import imbalances. Using NSGA-II optimization, the results highlight improved system sizing and reduced grid burden compared to traditional methods. The study by [11] highlights strategies for capacity allocation and stability maintenance in distribution networks. It identifies challenges and proposes solutions for competent energy use and grid stability. In [12], A new many input transformer linked with bidirectional converter is presented for a grid-linked PV-wind-battery system. The architecture reduces power conversion stages, improving efficiency and reliability. MATLAB simulations and experimental results demonstrate the system's capability in satisfying load demands, power injection, and battery management under diverse operational circumstances.

This paper investigates the application of an ANFIS-based MPPT algorithm for optimizing the performance of a grid-linked hybrid scheme with energy storage and EV integration. The system focuses on enhancing energy harvesting efficiency, reducing power quality issues such as THD, and ensuring effective energy management under dynamic operating conditions. By leveraging ANFIS-MPPT, the system achieves rapid and accurate tracking of optimal operating points, thereby addressing challenges associated with intermittent renewable energy sources. This research offers information on how to create and deploy cutting-edge hybrid systems that can satisfy contemporary grid demands.

II. SYSTEM DESCRIPTION

An integrated renewable energy system including a PV module, wind turbine, storage battery, and EV battery is depicted in Figure 1. The scheme is linked to the electrical grid and a centralized DC bus. An ANFIS MPPT controller ensures efficient power extraction when the PV array transforms sunlight into electrical energy. A boost converter receives the output to control and raise the voltage. In a similar manner, a P&O MPPT procedure monitors the MPP of the wind turbine, which produces electrical energy. For voltage control, a boost regulator is additionally attached to the wind turbine's output. The centralized DC bus receives its regulated DC power from both sources. The system uses bidirectional converters to connect an EV battery and a storage battery. These enable energy to move in both directions, either storing extra energy or returning it to the DC bus as required. The DC bus collects the energy from all sources and acts as the primary power distribution point. Before being sent to the grid, the DC power is transferred into AC via a three-phase DC-AC converter and filtered to enhance power quality. Maximum use of renewable energy, effective energy storage, and bidirectional power flow for EV charging and grid interaction are all guaranteed by the hybrid system.

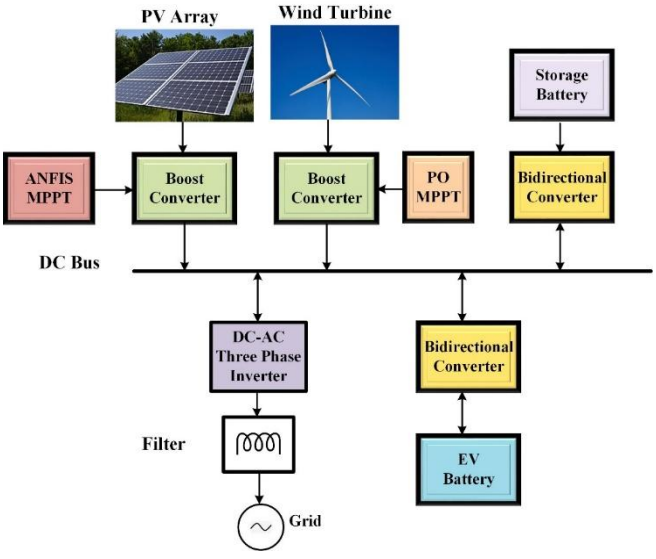

Fig.1 Representation of the Proposed Scheme

A. PV Model

The following equations can be used to characterize the mathematical representation for a PV panel:

$$I_{ph} = (I_{sc} + k_i(T - 298)) \times \frac{I_r}{1000} \quad (1)$$

where T is the temperature, I_r is the sun irradiation, K_i is the SC current's temperature coefficient, and I_{sc} is the SC current.

$$I_{rs} = I_o \left[\frac{T}{T_r}\right]^3 exp\left[\frac{q \times E_{go}}{nk}\left(\frac{1}{T} - \frac{1}{T_r}\right)\right] \quad (2)$$

where I_o represents the saturation current, Tr represents the nominal temperature, E_{go} signifies the semiconductor's band gap energy q signifies the electron charge, n is the diode's factor, and k represents Boltzmann's constant.

$$I = N_p \times I_{ph} - N_p \times I_o \left[exp\left(\frac{\frac{V}{N_S} + I \times \frac{R_S}{N_p}}{n \times V_t}\right) - 1\right] - I_{sh} \quad (3)$$

where V is the terminal voltage, N_S is the of cells linked in series, N is the number of PV modules connected in parallel, Rs & Rsh is the series & parallel resistance.

B. ANFIS MPPT

ANFIS incorporates fuzzy logic and ANN functions. The Sugeno-fuzzy controller is trained using an ANN to identify the precise MF for the variables based on their interdependencies. By determining the weights of the nodes involved, a thorough rule foundation may also be established. The model's inputs might be the PV array voltage and current or the PV irradiance and ambient temperature.

Layer 1- In this layer O1, node i's output is dependent upon the input of its corresponding node's membership functions. "I

$$O_1, i = \mu_{Ai}(x), for\ i = 1,2, \quad (4)$$

$$O_1, i = \mu_{Bi}(y), for\ i = 3,4, \quad (5)$$

Here, Ai and Bi are fuzzy sets in the parametric form connected to node I, while x and y are the inputs. Gaussian membership functions are employed in this study for the inputs x and y.

Layer 2- Nodes are fixed, and input functions determine the node I's output. This layer, known as the neural network layer.

$$O_2, i = \omega_i = \mu_{Ai}(x) * \mu_{Bi}(y), for\ i = 1,2, \quad (6)$$

Layer 3- Each and every node is fixed and identified by N. Since it is the total of the firing strengths of the rules from the preceding layer, the output of layer 3, O3, is referred to as standardized firing strengths.

$$O_3, i = \bar{\omega}_i = \frac{\omega_i}{\omega_1 + \omega_2}, for\ i = 1,2. \quad (7)$$

Layer 4- The parameters are as a result of the nodes' flexible properties. The parameters of this fuzzy logic node are {pi, qi, ri}.

$$O_4, i = \bar{\omega} f_i = \bar{\omega}_i(p_i x + q_i + r_i), for\ i = 1,2. \quad (8)$$

Layer 5- t has a single fixed node and computes its output as the sum of all incoming signals.

$$O_5, i = \sum_i \bar{\omega}_i f_i = \frac{\sum_i \omega_i f_i}{\sum_i \omega_i}, for\ i = 1,2. \quad (9)$$

C. PV MPPT Control using ANFIS

To assure effective power extraction and delivery to the DC bus, Fig. 2 shows a PV system with a boost regulator managed by a PI controller and MPPT based on the ANFIS. A boost regulator regulates the PV modules voltage and current, raising the PV potential to the necessary level. The PV array produces electricity based on temperature and solar irradiation.

Temperature and irradiance are inputs used by the ANFIS MPPT algorithm to determine the reference voltage (Vref) for the MPP. To modify the duty cycle of the boost regulator, the PI controller processes an error signal that is calculated by comparing the reference voltage with the actual PV voltage (Vpv). The control signal from the PI controller is converted into switching pulses for the switching element of the boost regulator using a PWM generator. The efficiency and responsiveness of the system are enhanced by this configuration, which guarantees that the PV array runs at its MPP in a variety of environmental circumstances and that the DC bus receives the optimal output for load or storage.

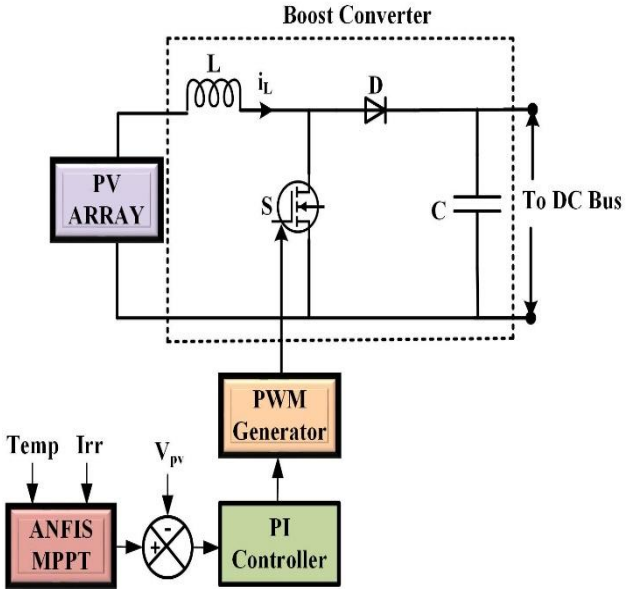

Fig.2 PV Control with ANFIS MPPT

D. Wind Turbine Modelling

The horizontal axis model is the most widely used due to its ability to capture maximum wind energy, adapt to low wind conditions, and adjust the pitch angle. The generator, comprises of gearbox and controllers, the

rotor, which has the blade and the frame, and the generator itself are therefore the three fundamental parts of a wind turbine.

$$P_{WT} = \begin{cases} 0, & v(t) \le v_{cutin} \ or \ v(t) \le v_{cutout} \\ P_r \frac{v(t)-v_{cutin}}{v_r - v_{cutout}}, & v_{cutin} < v < v_r \\ P_r, & v_r \le v(t) < v_{cutout} \end{cases} \quad (10)$$

According to the manufacturer, PWT is the WT's generated output power, v_r is its rated wind speed, and Pr is its rated power. The following equation shows how output power from WT may be more precisely calculated when hub height is taken into consideration.

$$V_2 = V_1 * \left(\frac{h}{h_{ref}}\right)^{\alpha} \quad (11)$$

The wind speed (V1 and V2) depends on the height of the hub (h), ref height (href), and the Wind gradient (α), typically set at 1/7. The output power of a WT is determined by the cut-in wind speed, rated wind speed, and cut-out wind speed.

E. PO MPPT for Wind

An iterative technique for determining the MPP in wind energy systems is the PO algorithm. First, the rotational speed (ω) of the generator and the output power (P) of the wind turbine are measured. The power converter's duty cycle or the generator speed are somewhat perturbed, which changes the operating point. Following the disturbance, the power change is examined by measuring the new output power (Pnew). The system is getting closer to the MPP if Pnew is higher than the prior power (Pprev), which causes more disturbance in the same direction. In contrast, the direction of perturbation is reversed if Pnew is less than P prev since the operating point is moving away from the MPP.

Based on the measured power variations, the algorithm continually modifies the generator's duty cycle or speed. For succeeding iterations, the current power P new is substituted for the prior power value Pprev. To ensure the best possible power extraction from the wind energy system, this procedure is repeated until the system stabilizes and achieves the maximum power point.

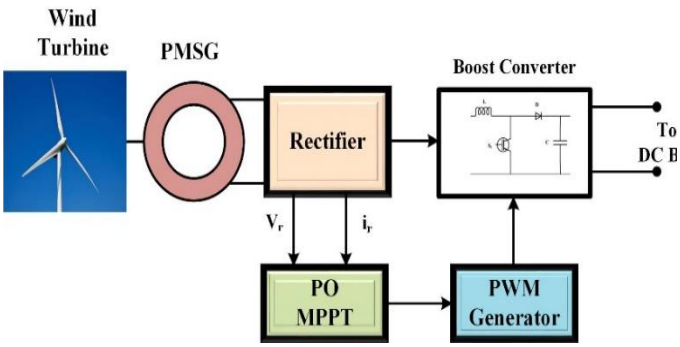

Fig.3 Wind control using PO MPPT

The wind energy conversion system depicted in Fig. 3 effectively converts and supplies energy to the DC bus by utilizing a wind turbine, PMSG, rectifier, boost regulator, and P&O MPPT algorithm. The wind turbine converts wind energy into mechanical energy, which powers the PMSG. The PMSG's AC power is transformed into DC electricity via the rectifier. The boost regulator receives the output voltage and current from the rectifier and increases the voltage to satisfy DC bus requirements. By varying the operating voltage and monitoring the resulting power, the P&O MPPT algorithm determines the wind energy system's MPP. It creates a reference signal for the PWM generator based on this. To ensure that the wind energy system runs as efficiently as possible, the PWM generator generates switching pulses to regulate the boost converter. After that, the DC bus receives the regulated DC power for use in loads or storage systems. Under various wind conditions, this configuration guarantees the best possible energy extraction and system stability.

F. Storage Battery

Because renewable energy sources are intermittent, energy storage devices are essential for applications involving them. The best option in this situation is battery-based storage. SOC is a crucial metric for controlling battery performance as it shows the proportion of accessible energy to the battery's overall energy storage capacity. P_{Batt} power of battery, $E_{Battmax}$ is the max energy stored , and E_{Batt} is the battery energy. The DC bus excess available power is known as P_{DCBus}, while the converter efficiency is known as $\eta_{BDC/DC}$. Furthermore, η_{dis} and η_{ch} are regarded as the discharge and charge efficiency of batteries, respectively. A recursive algorithm is used to determine the battery's energy at each instant.

$$Soc(t) = \frac{E_{bat}(t)}{E_{batmax}} \quad (12)$$

$$E_{bat}(t) = \int_{t-1}^{t} P_{bat}(t) \times \Delta t \quad (13)$$

$$E_{bat}(t) = E_{bat}(t-1) + \Delta E_{bat} \quad (14)$$

$$\Delta E_{bat} = \begin{cases} P_{dcbus} \times \eta_{ch} \times \eta_{bdc}, & where \ \delta > 0 \\ \frac{P_{dcbus}}{\eta_{dis} \times \eta_{bdc}}, & where \ \delta < 0 \\ 0, & where \ \delta = 0 \end{cases} \quad (15)$$

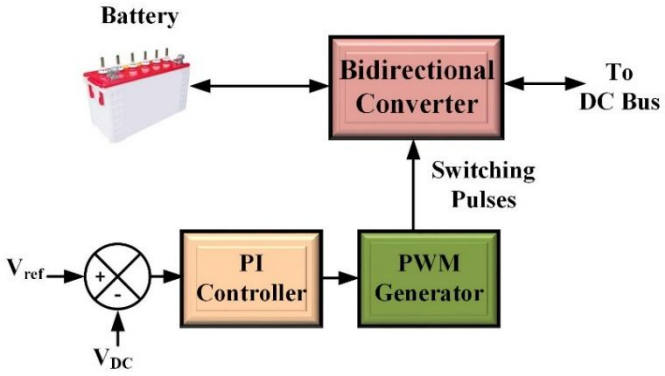

Fig.4 Battery Control

A battery storage system with a bidirectional regulator incorporated for DC bus voltage stability is controlled and operated as shown in Fig. 4. Through the bidirectional converter, energy exchange with the DC bus is made possible by the battery acting as the energy storage medium. The converter may operate in either charging mode, storing energy in the battery, or discharging mode, which provides energy to the DC bus, depending on the power requirements. A PI controller regulates the DC bus voltage by comparing it to a reference voltage. The PI controller processes the resulting error signal to keep the voltage level at the desired level. The switching pulses needed to operate the bidirectional converter are produced by the PWM generator, which is powered by the PI controller's output. To guarantee effective energy transfer between the battery and the DC bus and stabilize the system under various load circumstances, these switching pulses control the converter's duty cycle and operating mode.

G. Inverter Control

The control logic for an inverter in a RES is displayed in Fig. 5. The control system makes sure that the energy from the storage battery and the power produced by renewable resources (wind and PV) are effectively supplied to the load or grid. The total power available is first determined by adding the power inputs from the wind turbine and PV system . The extra power needed, if any, for charging or discharging the battery is calculated by subtracting the battery's SOC from a reference value. A PI controller processes the error signal to produce a control signal after comparing the resultant total reference current with the actual current. To ensure compatibility with the inverter's switching control, the PI controller's output is transformed from the dq0 reference frame to the abc frame. This signal is then used by a PWM generator to provide switching pulses for the inverter. The inverter can effectively control power flow, synchronize with the grid, and sustain steady operation thanks to this procedure. The overall layout guarantees that the system will function at its best while satisfying load requirements and preserving the condition of the battery.

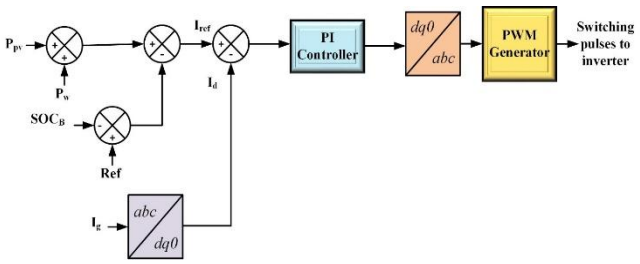

Fig.5 Inverter control using PI Controller

III. RESULTS & DISCUSSIONS

The system simulation is performed in MATLAB/Simulink. In this work, a 23.44 kW PV panel is used in this scheme, Here the PV operates at varying irradiance condition from 1000 W/m2 to 300 W/m2 decreased gradually. The PV parameters is denoted in the Fig.6.

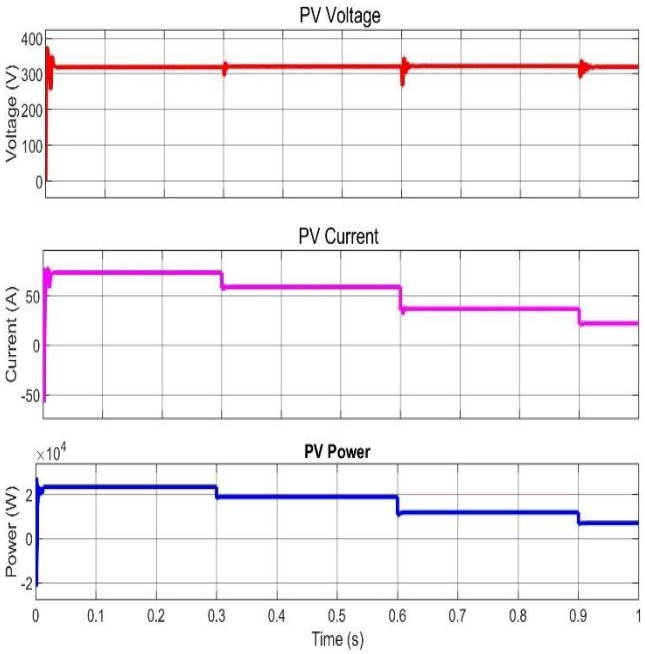

Fig.6 PV Parameters using ANFIS MPPT

Table.1 Efficiency of PV using ANFIS MPPT

Irradiance (W/m2)	Theoretical power (W)	Power Obtained (W)	Efficiency
1000	23.44	23.42	99.91
800	18.89	18.88	99.95
500	11.88	11.86	99.83
300	7.08	7.06	99.72

Table.1 presents the efficiency of a PV system utilizing the ANFIS-based MPPT technique under varying irradiance levels. At an irradiance of 1000 W/m^2, the theoretical power is 23.44 W, while the power obtained is

Doi: https://doi.org/10.XXXXX/IJDTSC.2025.V1I101

23.42 W, achieving an efficiency of 99.91%. Similarly, at 800 W/m^2, the theoretical power is 18.89 W, and the power obtained is 18.88 W, resulting in an efficiency of 99.95%. For lower irradiance levels, such as 500 W/m^2 and 300 W/m^2, the efficiencies are slightly lower but remain high at 99.83% and 99.72%, respectively. This demonstrates the effectiveness of the ANFIS MPPT technique in maintaining optimal performance across varying irradiance conditions.

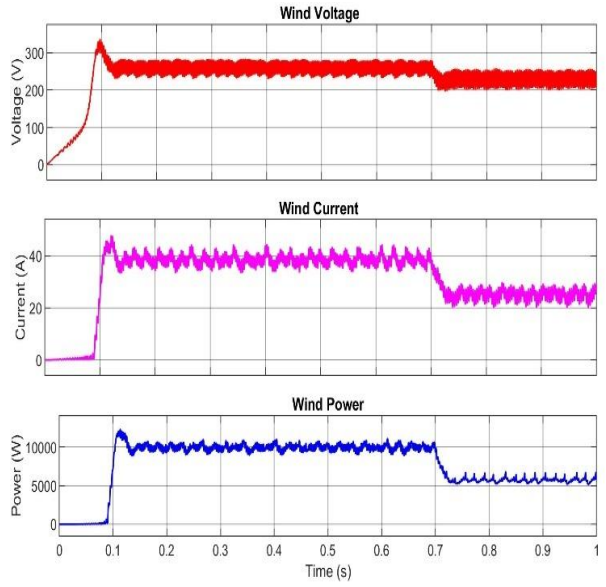

The Wind parameters are represented in Fig.7, Here the Wind turbine is operated at 12 m/s from 0 to 0.7 s & then is it reduced to 10 m/s, the power obtained by the wind is 9.59 kW & 6.20 kW respectively.

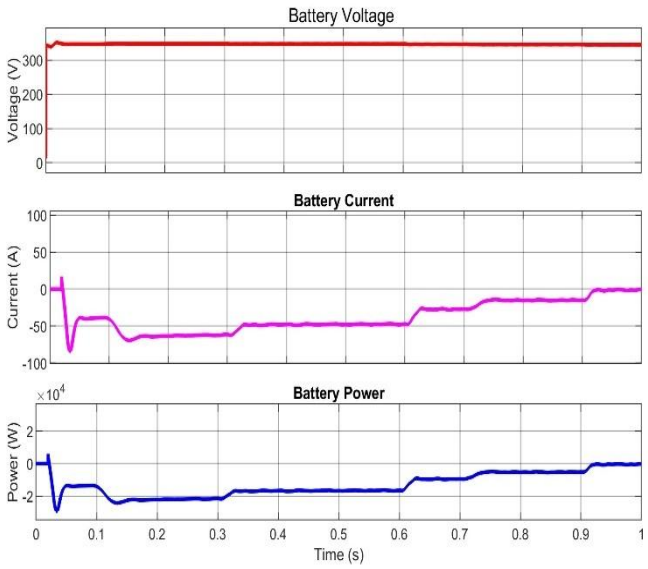

Fig.8 Parameters of Storage battery

The SB parameters are represented in Fig.8, It is inferenced that the battery power is varying according to the change in the input PV & wind power, When the input power reduced the charging state of the battery varies, when the input power is zero the SB supplied power to the EV Battery. The EV battery is represented in Fig.9. The EV battery receives continues power from the input sources & grid, even if the power from the source varies. The variation in the grid power according to the change in the input sources is represented in Fig.10. The grid receives power from the input sources up to 0.6s & then the grid supplies power to the EV battery to compensate for the insufficient power due to less irradiance in PV & Wind power.

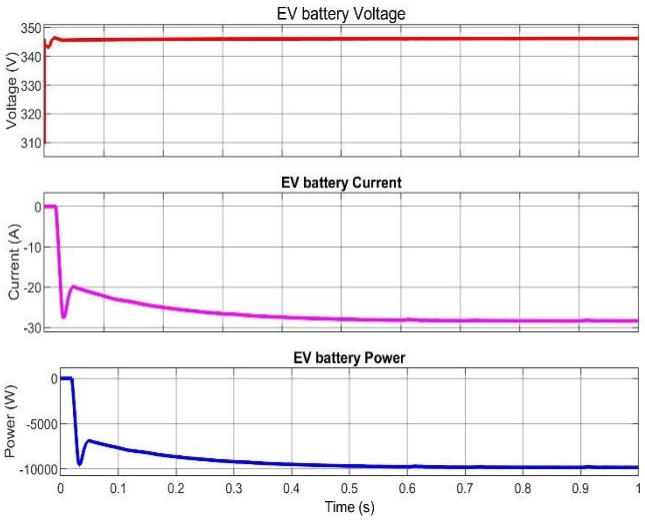

Fig.9 Parameters of EV Battery

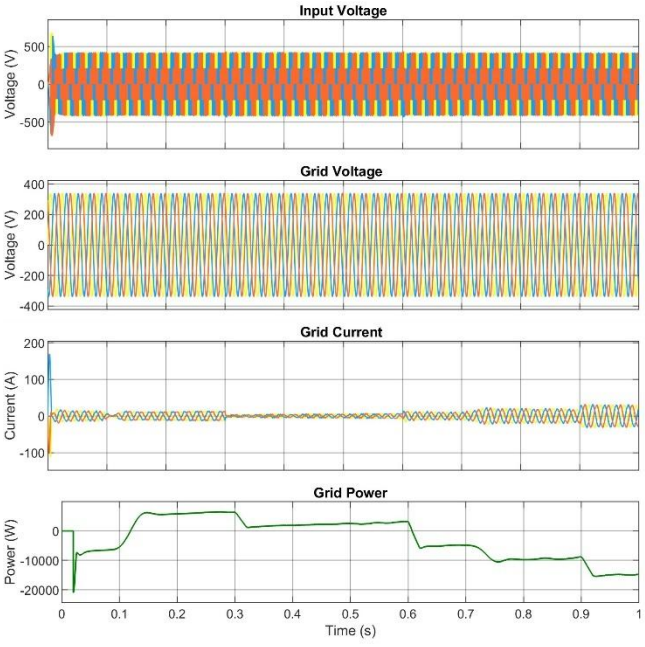

Fig.10 Parameters of Grid

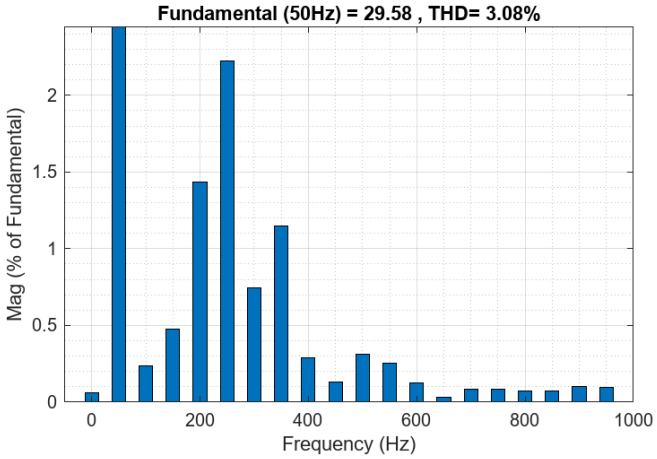

Fig.10 THD of the grid Current

The THD analysis of the grid current is presented in Fig.10. Here the THD is 3.08%, Which is less and meet the IEEE 519 standards.

IV. CONCLUSION

The Proposed scheme effectively maximizes energy harvesting from PV and wind subsystems under varying environmental conditions while maintaining high efficiency. The PV subsystem achieves efficiencies above 99.7% across irradiance levels from 1000 W/m^2 to 300 W/m^2, highlighting the superior performance of the ANFIS MPPT algorithm. The wind turbine delivers stable power outputs at varying wind speeds, ensuring reliable energy production. Energy storage plays a key role by stabilizing the system during fluctuations in renewable energy output. The storage battery adjusts its charging and discharging state based on variations in PV and wind power, providing a consistent supply to the EV battery during reduced input conditions. The EV battery ensures uninterrupted operation by receiving power from renewable sources and the grid. When renewable energy generation is insufficient, the grid compensates by supplying power to maintain system stability and meet demand. Simulation results confirm the system's capability to enhance power quality through reduced THD obtained is 3.08% and improved voltage regulation during grid disturbances.

REFERENCES

[1] Chakir, A., & Tabaa, M. (2024). Hybrid Renewable Production Scheduling for a PV–Wind-EV-Battery Architecture Using Sequential Quadratic Programming and Long Short-Term Memory–K-Nearest Neighbors Learning for Smart Buildings. Sustainability, 16(5), 2218.

[2] Aloo, L. A., Kihato, P. K., Kamau, S. I., & Orenge, R. S. (2023). Modeling and control of a photovoltaic-wind hybrid microgrid system using GA-ANFIS. *Heliyon*, *9*(4).

[3] Prabu, V. D., Sridevi, R., Karunakaran, M., & Suresh, V. (2024, August). HRES based Battery System with Optimal ANFIS-MPPT for Microgrid Applications. In 2024 7th International Conference on Circuit Power and Computing Technologies (ICCPCT) (Vol. 1, pp. 1710-1716). IEEE

[4] Hemanand, T., Subramaniam, N. P., & Venkateshkumar, M. (2018). Comparative analysis of intelligent controller based microgrid integration of hybrid PV/wind power system. Journal of Ambient Intelligence and Humanized Computing, 1-20.

[5] Singh, A. K., & Saxena, A. (2020). A novel neuro-fuzzy control scheme for wind-driven DFIG with ANN-controlled solar PV array. Environment, Development and Sustainability, 22(7), 6605-6626..

[6] Fungo, L. J., Mushi, A. T., & Msigwa, C. J. (2021, November). Grid connected pv-wind energy system for luxmanda village in tanzania. In The Third Annual Conference on Research and Inclusive Development (p. 86).

[7] Gulzar, M. M., Iqbal, A., Sibtain, D., & Khalid, M. (2023). An innovative converterless solar PV control strategy for a grid connected hybrid PV/wind/fuel-cell system coupled with battery energy storage. IEEE Access, 11, 23245-23259.

[8] Maaruf, M., Khan, K., & Khalid, M. (2022). Robust control for optimized islanded and grid-connected operation of solar/wind/battery hybrid energy. Sustainability, 14(9), 5673.

[9] Bokopane, L., Kusakana, K., Vermaak, H., & Hohne, A. (2024). Optimal power dispatching for a grid-connected electric vehicle charging station microgrid with renewable energy, battery storage and peer-to-peer energy sharing. Journal of Energy Storage, 96, 112435

[10] Niveditha, N., & Singaravel, M. R. (2022). Optimal sizing of hybrid PV–Wind–Battery storage system for Net Zero Energy Buildings to reduce grid burden. Applied Energy, 324, 119713.

[11] Yao, M., Da, D., Lu, X., & Wang, Y. (2024). A review of capacity allocation and control strategies for electric vehicle charging stations with integrated photovoltaic and energy storage systems. World Electric Vehicle Journal, 15(3), 101.

[12] Mangu, B., Akshatha, S., Suryanarayana, D., & Fernandes, B. G. (2016). Grid-connected PV-wind-battery-based multi-input transformer-coupled bidirectional DC-DC converter for household applications. IEEE journal of emerging and selected topics in power electronics, 4(3), 1086-1095.